



Heriot-Watt University
Research Gateway

Finite-dimensional coagulation-fragmentation dynamics

Citation for published version:

Carr, J, Al Ghamdi, M & Duncan, DB 2018, 'Finite-dimensional coagulation-fragmentation dynamics', *Mathematical Models and Methods in Applied Sciences*, vol. 28, no. 05, pp. 851-868.
<https://doi.org/10.1142/S0218202518500227>

Digital Object Identifier (DOI):

[10.1142/S0218202518500227](https://doi.org/10.1142/S0218202518500227)

Link:

[Link to publication record in Heriot-Watt Research Portal](#)

Document Version:

Peer reviewed version

Published In:

Mathematical Models and Methods in Applied Sciences

Publisher Rights Statement:

Electronic version of an article published in *Mathematical Models and Methods in Applied Sciences*, 28, 5, 2018, 851-868 DOI:10.1142/S0218202518500227 © World Scientific Publishing Company
[<http://www.worldscientific.com/worldscinet/m3as>]

General rights

Copyright for the publications made accessible via Heriot-Watt Research Portal is retained by the author(s) and / or other copyright owners and it is a condition of accessing these publications that users recognise and abide by the legal requirements associated with these rights.

Take down policy

Heriot-Watt University has made every reasonable effort to ensure that the content in Heriot-Watt Research Portal complies with UK legislation. If you believe that the public display of this file breaches copyright please contact open.access@hw.ac.uk providing details, and we will remove access to the work immediately and investigate your claim.

Finite Dimensional Coagulation Fragmentation Dynamics

Jack Carr*, Matab Alghamdi† and Dugald B Duncan‡

December 4, 2017

Abstract

We examine a finite dimensional truncation of the discrete coagulation-fragmentation equations that is designed to allow mass to escape from the system into clusters larger than those in the truncated problem. The aim is to be able to model within a finite system the process of gelation, which is a type of phase transition observed in aerosols, colloids etc.. The main result is a centre manifold calculation that gives the asymptotic behaviour of the truncated model as time $t \rightarrow \infty$. Detailed numerical results show that truncated system solutions are often very close to this centre manifold, and the range of validity of the truncated system as a model of the full infinite problem is explored for systems with and without gelation. The latter cases are mass conserving, and we provide an estimate using quantities from the centre manifold calculations of the time period the truncated system can be used for before loss of mass is apparent. We also include some observations on how numerical approximation can be made more reliable and efficient.

Keywords: coagulation-fragmentation dynamics, centre manifold.

1 Introduction

Consider a system of a large number of clusters of particles. The particles consist of an integer number of monomers and we can scale the mass so that the mass of the monomer is 1. The mass of a j -cluster consisting of j monomers is then j . The equations are used to model phenomena including particles suspended in the atmosphere, colloids, polymers and recently, telomere length maintenance in chromosomes, see §4.2 and [12].

The clusters can coagulate to form larger clusters or fragment to form smaller ones. Let $c_j(t) \geq 0$ be the concentration of clusters of size j . The coagulation-fragmentation equations are for $j = 1, 2, \dots$

$$c'_j = \frac{1}{2} \sum_{k=1}^{j-1} W_{j-k,k} - \sum_{k=1}^{\infty} W_{jk}, \quad c_j(0) \geq 0 \quad (1.1)$$

*1948–2016;

†Department of Mathematics, Faculty of Sciences, Jazan University, Saudi Arabia
malghamdi@jazanu.edu.sa;

‡Address for correspondence: Maxwell Institute for Mathematical Sciences, Department of Mathematics, Heriot-Watt University, Edinburgh, EH14 4AS, UK. D.B.Duncan@hw.ac.uk

where a prime denotes $\frac{d}{dt}$ and $W_{jk} = a_{jk}c_jc_k - b_{jk}c_{j+k}$. The constants $a_{j,k} \geq 0$ are the coagulation coefficients while the constants $b_{j,k} \geq 0$ are the fragmentation coefficients. We assume that $a_{j,k}$ and $b_{j,k}$ are symmetric.

The mass of clusters of size j at time t is $jc_j(t)$. The total mass or density of the system is then

$$M_1(t) = \sum_{j=1}^{\infty} jc_j(t). \quad (1.2)$$

In the derivation of the model (1.1), for each coagulation and fragmentation event the total mass is conserved, so we might expect that $M_1(t)$ is constant. In certain circumstances however, the density decreases. The mathematical reason is that larger and larger clusters are forming which escape to infinity. Physically this is interpreted as some of the particles being transferred to a new phase. This mass loss is known as gelation. The question of when gelation occurs depends on the kinetic coefficients $a_{j,k}$ and $b_{j,k}$ as well as the initial data.

As an example of gelation, consider the case $a_{j,k} = jk$, $b_{j,k} = 0$ and initial data $c_j(0) = \delta_{j,1}$. The solution [13, 14] is

$$c_j(t) = \begin{cases} \frac{j^{j-3} t^{j-1} e^{-jt}}{(j-1)!} & 0 \leq t \leq 1, \\ \frac{c_j(1)}{t} & t > 1. \end{cases} \quad (1.3)$$

Also,

$$M_1(t) = \begin{cases} 1 & t \leq 1, \\ \frac{1}{t} & t > 1. \end{cases} \quad (1.4)$$

The loss of mass at time $t = 1$ is associated with the formation of an infinite cluster. We also note that the second moment is given by

$$M_2(t) = \sum_{j=1}^{\infty} j^2 c_j(t) = (1-t)^{-1}$$

and this becomes infinite at the gelation point $t = 1$.

This paper studies a finite dimensional system which is often used to numerically solve (1.1). The n -dimensional truncation that we study is

$$\dot{c}_j = \frac{1}{2} \sum_{k=1}^{j-1} W_{j-k,k} - \sum_{k=1}^{n-j} W_{jk} - \sum_{k=n-j+1}^n a_{jk}c_jc_k, \quad c_j(0) \geq 0 \quad (1.5)$$

for $j = 1, 2, \dots, n$. The approximation is well suited to studying gelation since the density $M_1(t)$ is non-increasing. The reasons for the choice of truncation are discussed in the next section.

Figure 1 shows results from the truncated system (1.5) for the pure coagulation example above with $a_{j,k} = jk$, $b_{j,k} = 0$ and initial data $c_j(0) = \delta_{j,1}$. The figure shows a sharp decrease in $M_1(t)$ at approximately $t = 1$ and the rate of decay is very close to that given by (1.4). Different system sizes are used, and the truncated system mass appears to converge to the exact gelation behaviour (1.4) as n increases.

In this paper we assume that detailed balance holds:

$$a_{j,k}Q_jQ_k = b_{j,k}Q_{j+k} \quad (1.6)$$

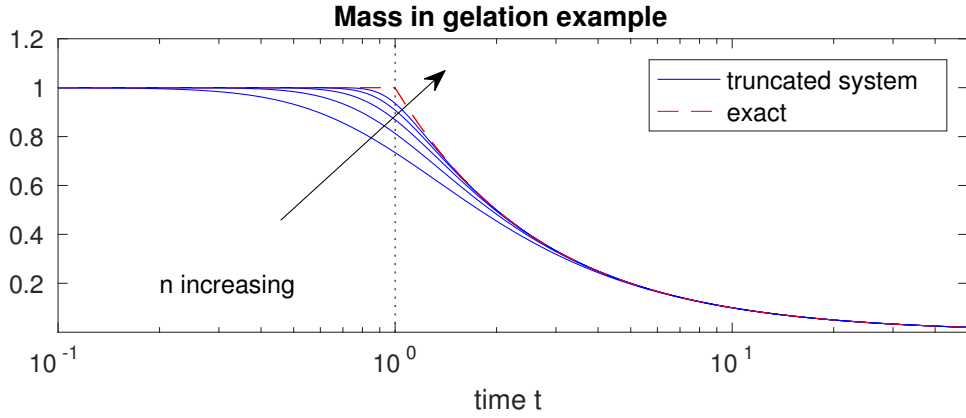


Figure 1: The mass in the truncated system (1.5) solution for $a_{j,k} = jk$, $b_{j,k} = 0$ and initial data $c_j(0) = \delta_{j,1}$ with maximum cluster sizes $n = 4, 8, 16, 32, 64$. The exact solution is given by (1.3) and the exact mass by (1.4).

for some $Q_j > 0$ with $Q_1 = 1$. The infinite system (1.1) has equilibrium solutions of the form

$$c_j = Q_j z^j, \quad j = 1, 2, \dots \quad (1.7)$$

with density $\sum_{j=1}^{\infty} j Q_j z^j$, as long as the series is finite. The only equilibrium solution to the finite dimensional problem (1.5) is the zero solution and all solutions of (1.5) converge to zero as $t \rightarrow \infty$. However, numerical studies show that for solutions of (1.5), the truncated density

$$M_1^n(t) = \sum_{j=1}^n j c_j(t) \quad (1.8)$$

decays very slowly. In fact, solutions seem to look like the equilibrium solutions (1.7). For small initial densities, we use centre manifold results to prove that for solutions of (1.5),

$$c_j(t) \approx Q_j (u(t))^j, \quad 1 \leq j \leq n \quad (1.9)$$

where

$$u(t) \approx \eta t^{-1/n} \quad (1.10)$$

with η a positive constant. Since the decay of (1.10) is very slow, this provides some explanation as to why in numerical calculations we see that solutions behave like equilibria and decay slowly. We also present some numerical solutions to support the above asymptotic results. For an earlier application of centre manifolds to the long time asymptotics of coagulation equations see [8].

2 Finite dimensional truncations

In order to develop a numerical scheme for solving coagulation-fragmentation equations of the form (1.1) we need to have a maximum size n for clusters. A natural way to do this is to solve the truncated system

$$\dot{c}_j = \frac{1}{2} \sum_{k=1}^{j-1} W_{j-k,k} - \sum_{k=1}^{n-j} W_{jk} \quad j = 1, 2, \dots, n. \quad (2.1)$$

The above system is often used for mathematical studies of (1.1). For example, see [2]. Existence of solutions to (1.1) is proved by solving (2.1) and letting $n \rightarrow \infty$. Solutions obtained in this way are called admissible and it is important to only consider this class of solutions since in general there are non-physical solutions to the infinite system [3, 10].

Solving (2.1) is a reasonable method for approximating solutions to the infinite system in certain cases. However, for (2.1) $\sum_{j=1}^n j c'_j = 0$ and so the truncated density M_1^n given by (1.8) is constant, which is not a useful property if we are studying gelation.

The truncated model (1.5) proposed here for numerical studies of (1.1) is derived in an analogous way to that of the truncation of a continuum coagulation-fragmentation equation in [1]. In both cases, truncation of the system is done such that coagulation allows for mass to be lost into larger clusters than are contained in the model, while these larger clusters are not allowed to fragment and feed mass back into the truncated system. We consider the truncated model (1.5) in more detail below.

First consider the pure coagulation case obtained with $b_{j,k} \equiv 0$ in (1.5):

$$c'_j = \frac{1}{2} \sum_{k=1}^{j-1} a_{j-k,k} c_{j-k} c_k - c_j \sum_{k=1}^n a_{j,k} c_k,$$

for $j = 1, 2, \dots, n$. This is the so-called “minimal n -truncation” of the pure coagulation version of (1.1) examined in [7]. It is called “minimal” because it sets to zero the smallest number of kinetic coefficients $a_{j,k}$ in (1.1), i.e. those with $\max(j, k) > n$. It models the coagulation interactions



for all cluster sizes $1 \leq j, k \leq n$. As the truncated system does not include clusters of size $j + k > n$, their mass is lost from the system and it is shown in [7, Prop. 3] that the truncated density M_1^n of this pure coagulation problem satisfies (2.2) below.

Second, consider the pure fragmentation case of (1.5) with $a_{j,k} \equiv 0$:

$$c'_j = \sum_{k=1}^{n-j} b_{j,k} c_{j+k} - \frac{c_j}{2} \sum_{k=1}^{j-1} b_{j-k,k},$$

for $j = 1, 2, \dots, n$. This is a “maximal n -truncation” in the nomenclature of [7], because it sets to zero the largest number of kinetic coefficients $b_{j,k}$ in (1.1), i.e. those with $j + k > n$. Clusters of size $> n$ are not allowed to fragment and to inject mass into the truncated system. It is relatively straightforward to show that $\sum_{j=1}^n j c'_j = 0$ here, and so the fragmentation process conserves the truncated density M_1^n .

Combining the results above for the coagulation-fragmentation truncated model (1.5) and assuming that all concentrations $c_j \geq 0$ gives

$$\frac{dM_1^n(t)}{dt} = - \sum_{j=1}^n \sum_{k=n-j+1}^n j a_{j,k} c_j c_k \leq 0. \quad (2.2)$$

The truncated density may be decreased by coagulation, but is unaffected by fragmentation. The non-increasing density property (2.2) is what we require to mimic gelling solutions in the infinite system (1.1).

Global existence of a unique solution to (1.5) with $c_j(t) \geq 0$ for all j is proved by standard arguments (see for example [3]). Suppose that the initial data are nonzero, that is, $c_k(0) > 0$ for some k . If some of the kinetic coefficients are zero, then some of the differential equations may decouple with $c_r(t) = 0$ for some r and all t . We make the simplest assumption which leads to the positivity of solutions. As well as the assumption (1.6) made about detailed balance we assume

$$a_{1,k} > 0, b_{1,k} > 0 \quad k \geq 1. \quad (2.3)$$

Theorem 2.1. *Assume (2.3), detailed balance (1.6) and let $c(t)$ be a solution to (1.5) with nonzero initial data. Then $c_j(t) > 0$ for all j and $t > 0$.*

Also, the only equilibrium solution of (1.5) is the zero solution and $c(t) \rightarrow 0$ as $t \rightarrow \infty$.

Proof. The positivity result was originally proved in [3, Theorem 4.2] for the infinite system (1.1). The proof is easily modified for the finite dimensional case (1.5).

Using the positivity of solutions and (2.3), $M_1^n(t)$ is a strictly decreasing Lyapunov function and the convergence result follows by standard arguments. \square

3 Asymptotics for the finite dimensional case

In this section we study the details of the large time behaviour of (1.5) under the assumptions that detailed balance (1.6) and positivity of coefficients (2.3) hold. Theorem 2.1 establishes that $c(t) \rightarrow 0$ as $t \rightarrow \infty$ and we use Centre Manifold theory (see e.g. [4, 11]) to study small solutions of (1.5) and their rate of decay to 0.

The general setting for centre manifold analysis around the zero solution following e.g. [4, 11] is to rearrange the system under consideration into the form

$$x' = Ax + f(x, y), \quad y' = By + g(x, y), \quad (3.1)$$

where $x \in \mathbb{R}^m, y \in \mathbb{R}^{n-m}$, square matrices A, B are constant, and f, g contain the non-linear terms. The eigenvalues of A must have real part 0, and those of B must have real part < 0 . We also need the nonlinear terms f, g and their Jacobian matrices Df, Dg to vanish at $(x, y) = (0, 0)$. Then from [4, Thm. 1] there exists $h(x) \in C^2$ such that $y = h(x)$ is an invariant manifold for (3.1) and $h(0) = 0, Dh(0) = 0$. Flow on the centre manifold is governed by the m dimensional system

$$u' = Au + f(u, h(u)) \quad (3.2)$$

and [4, Thm. 2] gives the asymptotic behaviour as $t \rightarrow \infty$

$$x(t) = u(t) + \mathcal{O}(e^{-\gamma t}), \quad y(t) = h(u(t)) + \mathcal{O}(e^{-\gamma t})$$

where $\gamma > 0$ is constant. Substituting $y(t) = h(x(t))$ into (3.1) and rearranging gives

$$Dh(x) (Ax + f(x, h(x))) = Bh(x) + g(x, h(x)), \quad (3.3)$$

an equation for h together with the conditions $h(0) = 0, Dh(0) = 0$. This is generally impossible to solve explicitly, but approximation of $h(x)$ in powers of x to high enough order is sufficient in what follows.

Now consider the problem (1.5). To establish the dimension of the centre and stable manifolds we write it as $c' = F(c)$ where $c, F \in \mathbb{R}^n$, and find the eigenvalues of the Jacobian matrix $DF(c)$ at $c = 0$. The matrix is

$$DF(0) = \left(\begin{array}{c|ccc} 0 & b_{1,1} & \dots & b_{1,n-1} \\ \hline 0 & & & B \end{array} \right)$$

where sub-matrix

$$B = \begin{pmatrix} -\gamma_1 & b_{2,1} & b_{2,2} & \dots & b_{2,n-2} \\ 0 & -\gamma_2 & b_{3,1} & \dots & b_{3,n-3} \\ \vdots & \ddots & \ddots & \ddots & \vdots \\ 0 & \dots & 0 & -\gamma_{n-2} & b_{n-1,1} \\ 0 & \dots & \dots & 0 & -\gamma_{n-1} \end{pmatrix} \quad (3.4)$$

with

$$\gamma_j = \frac{1}{2} \sum_{k=1}^{j-1} b_{j-k,k} \geq \frac{1}{2} b_{1,j-1} > 0 \quad (3.5)$$

from assumption (2.3). The eigenvalues of the upper triangular matrix $DF(0)$ are its diagonal elements $\{0, -\gamma_1, \dots, -\gamma_{n-1}\}$ and so from the Centre Manifold Theorem [11, Thm. 8.1] the zero solution has a centre manifold of dimension 1 (one eigenvalue with real part 0), and the dimension of the stable manifold is $n - 1$ (since there are $n - 1$ eigenvalues with real part < 0).

To carry out the analysis of (1.5) it is convenient to replace the equation for rate of change of monomer density by one for the rate of change of truncated density M_1^n from (1.8). We change variables from (c_1, c_2, \dots, c_n) to x, y where

$$y_r = c_r, \quad 2 \leq r \leq n \quad \text{and} \quad x = M_1^n = \sum_{r=1}^n r c_r. \quad (3.6)$$

We write $y = [y_2, y_3, \dots, y_n]^T$ so $y \in \mathbb{R}^{n-1}$. For ease of notation in writing down the equations we make use of $y_1 = y_1(x, y_2, y_3, \dots, y_n)$ defined by

$$y_1 = x - \sum_{r=2}^n r y_r. \quad (3.7)$$

The scalar y_1 is not part of the vector y .

Equations (1.5) can now be written in the centre manifold analysis form (3.1) as

$$x' = f(x, y), \quad y' = B y + g(x, y) \quad (3.8)$$

where $x \in \mathbb{R}^1$, $y \in \mathbb{R}^{n-1}$, $A = 0$, matrix B is as defined in (3.4), equation (2.2) gives

$$f(x, y) = - \sum_{j=1}^n j \sum_{k=n-j+1}^n a_{j,k} y_j y_k, \quad (3.9)$$

and $g : \mathbb{R}^n \rightarrow \mathbb{R}^{n-1}$ with components g_r , $r = 2, 3, \dots, n$. The components are given by

$$g_r(x, y) = \frac{1}{2} \sum_{k=1}^{r-1} a_{r-k,k} y_{r-k} y_k - \sum_{k=n-r+1}^n a_{r,k} y_r y_k, \quad (3.10)$$

with $y_1 = y_1(x, y)$ given by (3.7). The functions f, g clearly satisfy the required conditions $f(0, 0) = 0$, $g(0, 0) = 0$, $Df(0, 0) = 0$ and $Dg(0, 0) = 0$.

Theorem 3.1. *Assume detailed balance (1.6), positivity of coefficients (2.3) and let $c(t)$ be a solution to (1.5) with nonzero initial data which is not on the stable manifold. Define k_n by*

$$k_n = n \sum_{j=1}^n j a_{j,n-j+1} Q_j Q_{n-j+1}. \quad (3.11)$$

Then as $t \rightarrow \infty$,

$$c_j(t) = Q_j (k_n t)^{-j/n} (1 + o(1)), \quad j = 1, 2, \dots, n \quad (3.12)$$

Proof. We consider the equivalent problem (3.8). It follows from [4, Thm. 1] that there is a centre manifold $y = h(x)$ with $h : \mathbb{R} \rightarrow \mathbb{R}^{n-1}$. We write the components of h as h_r for $2 \leq r \leq n$. We also introduce the scalar

$$h_1(x) = x - \sum_{r=2}^n r h_r(x). \quad (3.13)$$

The equation on the centre manifold is, from (3.2) with $A = 0$ and (3.9),

$$u' = f(u, h(u)) = - \sum_{j=1}^n j \sum_{k=n-j+1}^n a_{j,k} h_j(u) h_k(u) \quad (3.14)$$

with h_1 defined by (3.13). Since $u' < 0$ we have that $u(t)$ will decay to zero as $t \rightarrow \infty$. We need a better approximation than $h(u) = \mathcal{O}(u^2)$ in order to find the decay rate. To do this we use [4, Thm. 3] and construct an approximation $\phi(u)$ of $h(u)$ with the required properties. Let $\phi : \mathbb{R} \rightarrow \mathbb{R}^{n-1}$ with $\phi(u) = \mathcal{O}(u^2)$ as $u \rightarrow 0$. We write the components of ϕ as ϕ_r for $2 \leq r \leq n$. We also define the scalar $\phi_1(u)$ by

$$\phi_1(u) = u - \sum_{r=2}^n r \phi_r(u). \quad (3.15)$$

We define

$$(M\phi)(u) = \phi'(u) f(u, \phi(u)) - B\phi(u) - g(u, \phi(u)) \quad (3.16)$$

so that $(Mh)(x) = 0$, a rearrangement of (3.3). Our aim is to choose ϕ so that $(M\phi)(u) = \mathcal{O}(u^q)$ for some $q > 2$ so that by centre manifold theory, $h(u) = \phi(u) + \mathcal{O}(u^q)$.

For each $u > 0$, let $z(u)$ be the unique solution of

$$u = \sum_{r=1}^n r Q_r (z(u))^r = z(u) + \sum_{r=2}^n r Q_r (z(u))^r,$$

so that

$$z(u) = u + \mathcal{O}(u^2) \quad \text{as } u \rightarrow 0 \quad (3.17)$$

where the Q_j are defined by the detailed balance relations (1.6).

We define $\phi(u)$ with components ϕ_r for $2 \leq r \leq n$ by $\phi_r(u) = Q_r (z(u))^r$. From (3.15) the scalar $\phi_1(u)$ is

$$\phi_1(u) = u - \sum_{r=2}^n r Q_r (z(u))^r = z(u).$$

Since $\phi_1(u) = z(u)$ and $Q_1 = 1$, we have that

$$\phi_r(u) = Q_r(z(u))^r, \quad 1 \leq r \leq n, \quad (3.18)$$

in the same form as the infinite system equilibrium solution (1.7). We show that with this choice of ϕ in (3.16),

$$(M\phi)(u) = \mathcal{O}(u^{n+1}). \quad (3.19)$$

We first estimate $\phi'(u)f(u, \phi(u))$. Now

$$f(u, \phi(u)) = - \sum_{j=1}^n j \sum_{k=n-j+1}^n a_{j,k} \phi_j(u) \phi_k(u).$$

In the above sum, $j+k \geq n+1$ and by (3.17) and (3.18), $\phi_r(u) = \mathcal{O}(u^r)$ for all r . It follows that $f(u, \phi)$ is of order

$$\sum_{j=1}^n \sum_{k=n-j+1}^n z^{j+k} = \mathcal{O}(u^{n+1}).$$

For $r \geq 2$,

$$\phi'_r(u) = rQ_r z^{r-1}(u) z'(u),$$

so that

$$\phi'(u)f(u, \phi(u)) = \mathcal{O}(u^{n+2}).$$

Next we estimate the r component of the second term of g in equation (3.10) which is

$$\sum_{k=n-r+1}^n a_{j,k} \phi_r(u) \phi_k(u).$$

Using $\phi_r(u) = \mathcal{O}(u^r)$ for all r , this term is of order

$$\sum_{k=n-r+1}^n z^{r+k} = \mathcal{O}(z^{n+1}).$$

The remaining terms in $B\phi + g(u, \phi(u))$ involve sums of terms $W_{j,k}$ with

$$W_{j,k} = a_{j,k} \phi_j \phi_k - b_{j,k} \phi_{j+k}$$

We show that all of these terms are zero. Using (3.18), for $j, k \geq 1$,

$$W_{j,k} = a_{j,k} Q_j Q_k z^{j+k} - b_{j,k} Q_{j+k} z^{j+k} = (a_{j,k} Q_j Q_k - b_{j,k} Q_{j+k}) z^{j+k} = 0$$

by detailed balance. This completes the proof of (3.19).

It follows that the components of the centre manifold h are given by

$$h_r(u) = Q_r(z(u))^r + \mathcal{O}(u^{n+1}), \quad (3.20)$$

for $r \geq 2$. From (3.13)

$$h_1(u) = u - \sum_{r=2}^n r Q_r(z(u))^r + \mathcal{O}(u^{n+1}) = z(u) + \mathcal{O}(u^{n+1}),$$

so that (3.20) holds for all r .

The equation (3.14) on the centre manifold is $u' = f(u, h(u))$, and using (3.20)

$$f(u, h(u)) = - \sum_{j=1}^n j \sum_{k=n-j+1}^n a_{jk} Q_j Q_k z^{j+k} + \mathcal{O}(u^{n+2}).$$

In the above sum, we only need to keep the terms with $j + k = n + 1$ since the others are $\mathcal{O}(u^{n+2})$. Hence

$$f(u, h(u)) = -u^{n+1} \sum_{j=1}^n j a_{j, n-j+1} Q_j Q_{n-j+1} + \mathcal{O}(u^{n+2}).$$

Since $u(t) \rightarrow 0$ as $t \rightarrow \infty$, the equation on the centre manifold may be written as

$$u' = -k_n n^{-1} u^{n+1} (1 + o(1)) \quad (3.21)$$

where k_n is defined by (3.11). Integrating the above equation,

$$u(t) = (k_n t)^{-1/n} (1 + o(1)). \quad (3.22)$$

It follows from Centre Manifold theory that for large t

$$x(t) = u(t) + \mathcal{O}(e^{-\gamma t}), \quad c_r(t) = h_r(u(t)) + \mathcal{O}(e^{-\gamma t}), \quad r \geq 2.$$

Using this together with (3.17), (3.20) and (3.22) proves the asymptotic relation (3.12) and this completes the proof of the theorem. \square

4 Examples

We consider the truncated system (1.5) applied to two different examples here. The first in Section 4.1 conserves density in the infinite system, and the second in Section 4.2 can undergo gelation. We examine how the asymptotic results of Theorem 3.1 relate to the numerical results. Some comments on the particular difficulties and details of the numerical approximation are given in Section 4.3.

4.1 Example 1: mass conserved in infinite system

We let $a_{jk} = b_{jk} = 1$ for all j, k , so that detailed balance holds with $Q_j = 1$ for all j . For this case, all admissible solutions of the infinite system (1.1) conserve density [3]. We approximate the solution of the truncated system (1.5) with initial data

$$c_1(0) > 0, \quad c_r(0) = 0, \quad r = 2, \dots, n. \quad (4.1)$$

Details of the numerical approximation are given in Section 4.3. Note that $c_1(0) = M_1^n(0)$, where $M_1^n(t)$ is defined by (1.8). Since these initial data are not on the stable manifold, Theorem 3.1 implies that

$$\lim_{t \rightarrow \infty} (k_n t)^{j/n} c_j(t) = 1$$

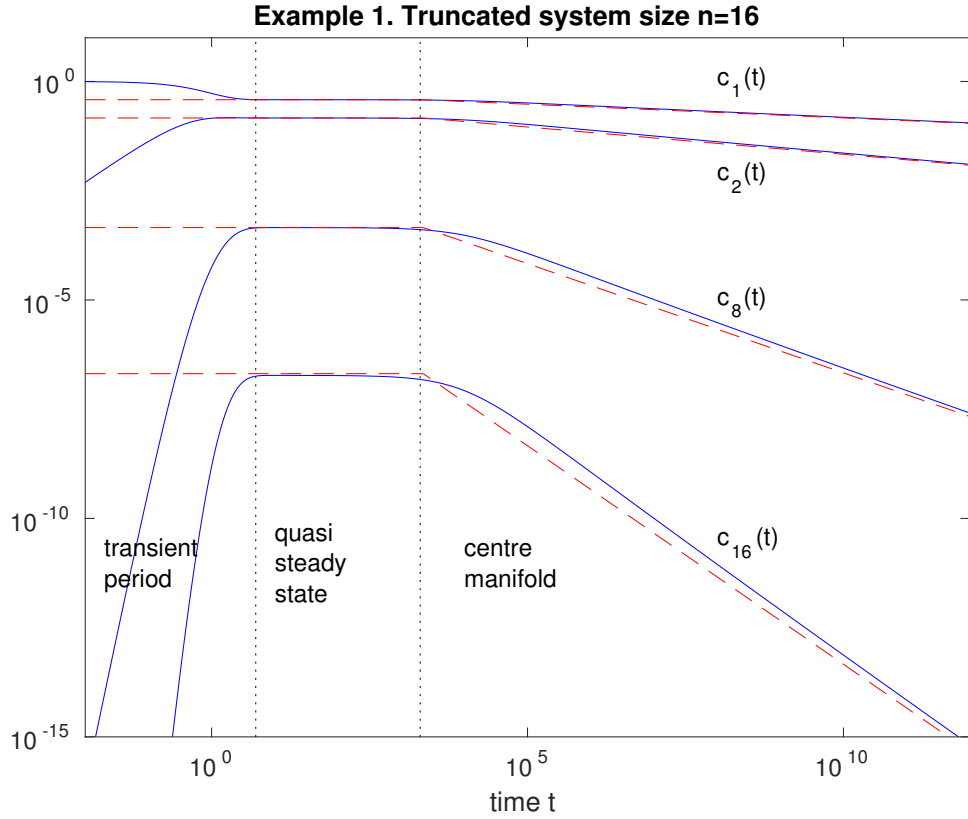


Figure 2: Comparison of actual concentrations, quasi steady state and centre manifold asymptotics for Example 1. The solid lines are the solution of the Example 1 problem with initial data (4.1) where $c_1(0) = 1$, and the dashed lines show the ∞ steady state values up to $t \approx 2000$, and then the asymptotic values $c_r(t) \approx (k_n t)^{-j/n}$ given in Theorem 3.1.

where

$$k_n = n \sum_{j=1}^n ja(j, n-j+1)Q_j Q_{n-j+1} = \frac{n^2(n+1)}{2}.$$

The other important time scale is given by the eigenvalues $-\gamma_r$ of matrix B defined by (3.5). This is related to the duration of the initial transient part of the solution. For this example $\gamma_r = (r-1)/2$ for $r = 2, \dots, n$, and so the initial transient should be damped out like $\mathcal{O}(e^{-t/2})$. We show results in Figure 2 for truncated system size $n = 16$ with $M_1(0) = 1$. We see that the initial transient lasts for about 10 time units, which is consistent with the predicted $\mathcal{O}(e^{-t/2})$ behaviour. After that the solution stays very close to the quasi steady state $c_j = z_n^j$, where

$$\sum_{j=1}^n j z_n^j = M_1(0)$$

for the given initial density $M_1(0) = 1$, and finally undergoes a long slow decay approaching the predicted centre manifold asymptotics

$$c_j(t) \approx (k_n t)^{-j/n}, \quad j = 1, \dots, n$$

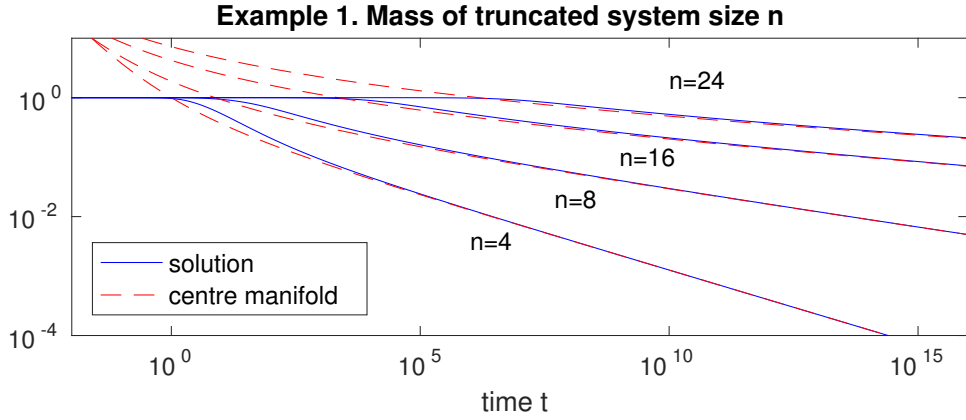


Figure 3: Comparison of truncated system mass (solid lines) with the approximate centre manifold mass $\sum_{j=1}^n j(k_n t)^{-j/n}$ for $n = 4, 8, 16, 24$ for Example 1 with initial data (4.1) where $c_1(0) = 1$.

quite clearly. In this case z_{16} is very close to the infinite steady state value

$$z_\infty = \frac{2M_1(0) + 1 - \sqrt{1 + 4M_1(0)}}{2M_1(0)},$$

and this is true whenever n is big enough.

The total mass in the truncated system of size $n = 16$ is almost conserved up to the end of the quasi steady state period shown on Figure 2, and then it decreases slowly as predicted by Theorem 3.1. This behaviour is replicated for bigger truncated systems, where the period the mass is conserved for increases, while the decay rate decreases. We show the total mass in the truncated system for different values of n in Figure 3. The mass conserving period also increases if the initial density is decreased. In these cases, if the initial transient has long enough to die away, then the intersection between the steady state concentrations $c_j(t) \approx z_\infty^j$ and the centre manifold asymptotic curves $c_j(t) \approx (k_n t)^{-j/n}$ gives a good indication of the timescale required for the mass loss to become apparent. This timescale grows exponentially with system size n and has the form

$$\text{apparent mass conservation period} = \mathcal{O}(k_n^{-1} z_\infty^{-n}) \quad \text{as } n \rightarrow \infty. \quad (4.2)$$

On Figure 3, $M_1(0) = 1$ and so $z_\infty \approx 0.38$. This shows up clearly on Figure 3 where the approximate centre manifold mass curves intersect the constant mass $M_1(t) = 1$ line close to where the solution mass starts to be visibly reduced.

Details of the length of this period of approximate mass conservation in Example 1 can also be seen in the upper plot of Figure 4 where different system sizes are compared. If we choose density $M_1(0)$ then the intersection of the the horizontal line $M_1(t) = M_1(0)$ with the appropriate approximate centre manifold mass curve for different system sizes n gives a good estimate of its duration. If we fix n and change $M_1(0)$, then the same process indicates that the duration increases as $M_1(0)$ decreases.

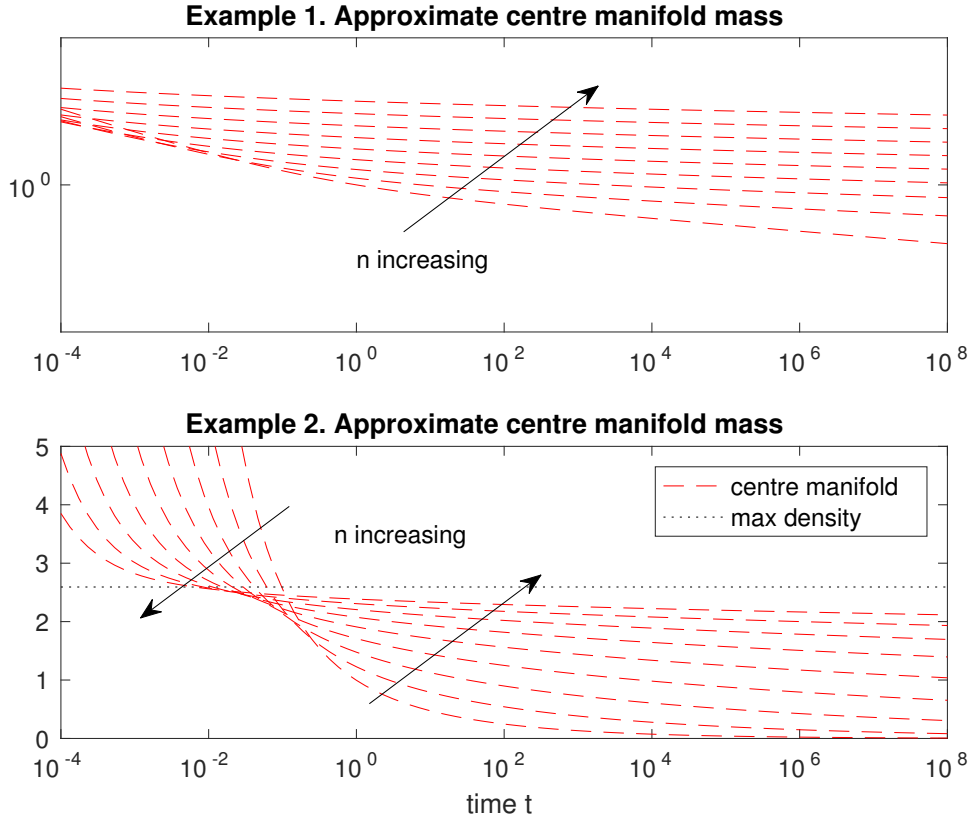


Figure 4: Mass on the approximate centre manifold $c_j(t) = Q_j(k_n t)^{-j/n}$ given in Theorem 3.1 for system sizes $n = 4, 8, 16, \dots, 1024$. The parameters in Example 2 are $\alpha = 1.5$ and $b_0 = 1$ and the maximum equilibrium density (4.4) is shown as a horizontal dotted line.

4.2 Example 2: gelation possible in infinite system

This example is motivated by a model of length regulation in telomeres [12] where

$$a_{jk} = jk, \quad b_{jk} = \frac{b_0(j+k)^{\alpha+1}}{(jk)^\alpha} \quad (4.3)$$

with $\alpha = 1.5$ and $b_0 = 1$. Gelation can occur in the infinite system defined by these rates.

We consider the more general case with $b_0 > 0$ and $\alpha \geq 0$ in (4.3). This satisfies the detailed balance condition with

$$Q_j = b_0^{1-j} j^{-(\alpha+1)}$$

and equilibrium solutions are given by $c_j = Q_j z^j$ with density

$$F(z) = \sum_{j=1}^{\infty} j Q_j z^j = b_0 \sum_{j=1}^{\infty} j^{-\alpha} \left(\frac{z}{b_0} \right)^j.$$

The radius of convergence of the above series is $z = b_0$ with $F(b_0)$ finite if and only if $\alpha > 1$. Hence if $\alpha \leq 1$ we have equilibrium solutions of all densities, while if $\alpha > 1$

$$\bar{M}_1 = b_0 \sum_{j=1}^{\infty} j^{-\alpha} \quad (4.4)$$

is the maximum equilibrium density. We do not show results for $\alpha \leq 1$ here because they look very similar to the mass conserving results of Example 1: an initial transient period, then a quasi steady state followed by slow decline on the centre manifold.

If $b_0 = 0$, so that there is no fragmentation, then all nonzero solutions of (1.1) have gelation [13]. Since fragmentation reduces the rate of formulation of large clusters, if the fragmentation is strong enough then solutions should conserve density. If $\alpha < 1$ this is the case; all admissible solutions conserve density [6, Theorems 5.1 and 5.2].

We now consider the case $\alpha > 1$ with b_0 fixed. There are density conserving equilibrium solutions with density not greater than \bar{M}_1 given by (4.4). We give a formal proof that we always have gelation if the initial density $M_1(0)$ is large enough. The formalities could be made rigorous using the methods in [9, Section 6].

We write $M_p(t) = \sum_{j=1}^{\infty} j^p c_j(t)$ for the p -moment of a solution c to (1.1). A formal calculation shows that

$$M_0'(t) = -\frac{M_1^2(t)}{2} + \frac{1}{2} \sum_{j,k} b_{jk} c_{j+k}(t). \quad (4.5)$$

We can write the second term in (4.5) as

$$\frac{1}{2} \sum_{r=2}^{\infty} u_r c_r$$

with

$$u_r = \sum_{j=1}^{r-1} b_{r-j,j} = br^{\alpha+1} \sum_{j=1}^{r-1} (j(r-j))^{-\alpha}.$$

Suppose that we can show that u_r is less than a constant multiple of r . From (4.5)

$$M_0'(t) \leq -\frac{M_1(t)}{2} (M_1(t) - C), \quad (4.6)$$

for some constant $C > 0$. If $M_1(t)$ is constant, then for large enough $M_1(0)$ the right hand side of (4.6) is negative so that $M_0(\bar{t}) = 0$ for some $\bar{t} > 0$. This is a contradiction and would show that we have gelation.

We now prove the bound on u_r . By symmetry

$$\sum_{j=1}^{r-1} (j(r-j))^{-\alpha} = 2 \sum_{j=1}^{\lfloor r/2 \rfloor} j^{-\alpha} (r-j)^{-\alpha}, \quad (4.7)$$

where $\lfloor r/2 \rfloor$ is the smallest integer greater than (or equal) to $r/2$. Also, for $1 \leq j \leq \lfloor r/2 \rfloor$,

$$(r-j)^{-\alpha} \leq (\text{constant}) r^{-\alpha}.$$

Since $\alpha > 1$ the series

$$\sum_{j=1}^{\infty} j^{-\alpha},$$

is convergent. It follows that the series in (4.7) is bounded by a constant multiple of $r^{-\alpha}$ so from (4.5) we have

$$u_r \leq (\text{constant}) r$$

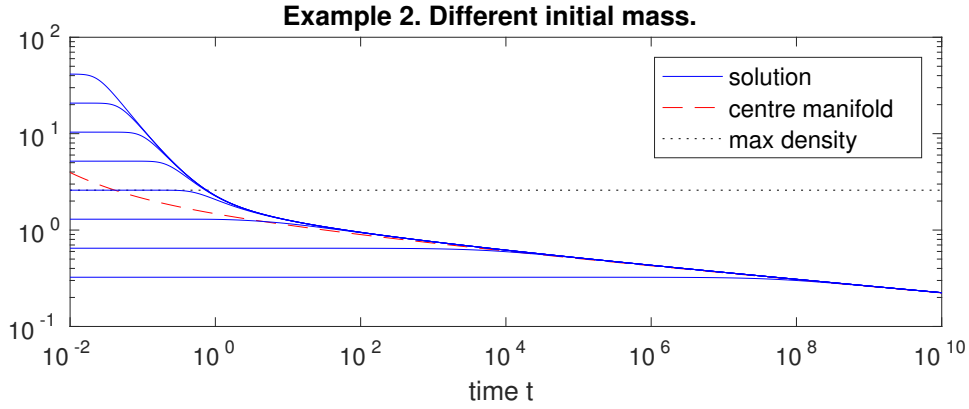


Figure 5: Mass versus time in the solution of the truncated system with $n = 16$ for Example 2 with $\alpha = 1.5$, $b_0 = 1$, initial data (4.1) and different initial masses. The maximum equilibrium density (4.4) is shown on the plot, along with the mass in the approximate centre manifold.

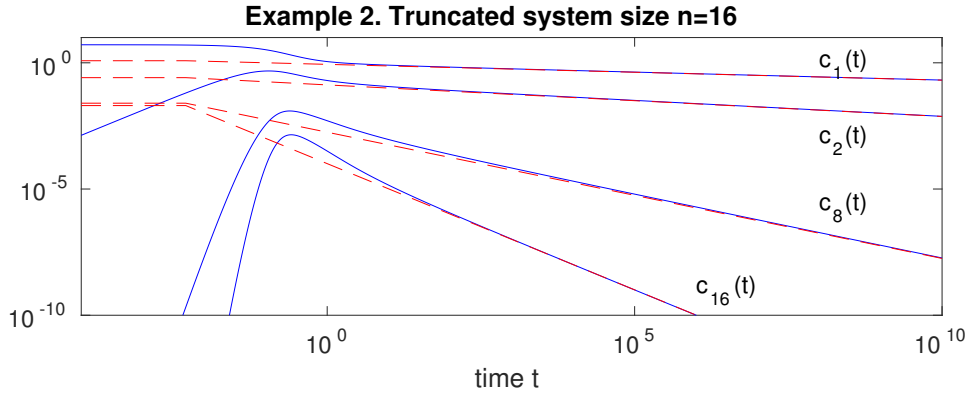


Figure 6: Solution components for truncated system size $n = 16$ for Example 2 with $\alpha = 1.5$, $b_0 = 1$, initial data (4.1) with $c_1(0) \approx 5.18$, twice the maximum equilibrium density (4.4). The dashed lines show the centre manifold asymptotic values $c_r(t) \approx Q_j(k_n t)^{-j/n}$ predicted by Theorem 3.1 with the short horizontal sections at the left showing the steady state values.

as required. This shows that we have gelation if $\alpha > 1$ with $b_0 > 0$ fixed and initial data with large enough density $M_1(0)$. A simple scaling argument shows that we also have gelation for fixed $M_1(0)$ if b_0 is large enough.

In Figure 5 we show results of Example 2 for fixed system size, α and b_0 and different initial masses. The behaviour when the mass is below the maximum equilibrium density is essentially the same as for Example 1: an initial transient period, a quasi steady state followed by a slow decay on the centre manifold. However when the initial mass is higher, we see in Figure 6 that the initial transient period leads straight into the centre manifold decay.

In Figure 7 we fix the initial mass at a level significantly above the maximum equilibrium density so that we expect gelation, and plot the system mass against time for different system sizes n . The period of apparent mass conservation increases with n and appears to converge to $t \approx 0.25$ which presumably corresponds to the time when gelation occurs. Examining the results over a longer time period again confirms a very good match with the centre manifold asymptotic results.

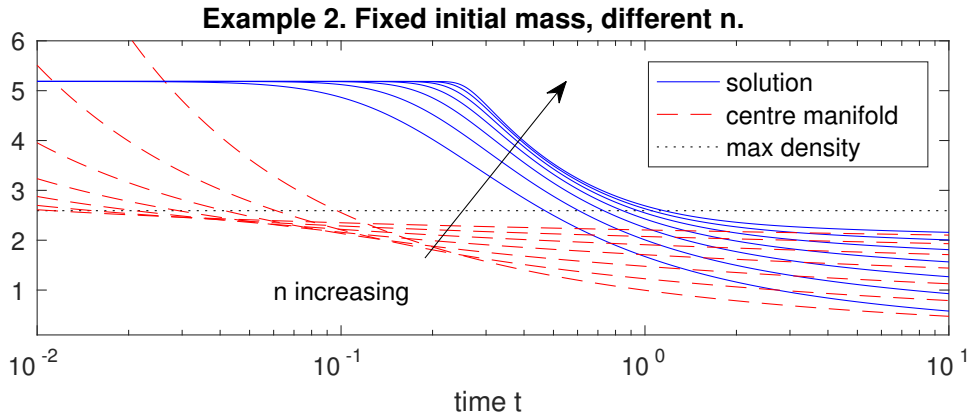


Figure 7: Example 2 with $\alpha = 1.5$, $b_0 = 1$, initial data (4.1) with $c_1(0) \approx 5.18$, twice the maximum equilibrium density (4.4). The solid lines show the mass in truncated systems of size $n = 4, 8, 16, \dots, 256$ and the dashed lines show the mass on the approximate centre manifold.

4.3 Numerical approximation

The ODE system (1.5) in the previous examples can be very stiff, even when the system size n is small. By “stiff” we mean that there is a high contrast in the timescales present, which causes stability problems for numerical ODE solvers and makes explicit methods useless. This stiffness is to be expected given that the analysis reveals different timescales: slow behaviour on the centre manifold; and a fast collapse of solutions onto the centre manifold. The contrast measured by the ratio of the largest to smallest eigenvalue of the Jacobian matrix for the ODE system (all are real and negative in the cases of interest) is many orders of magnitude, and can increase as the solution evolves along the centre manifold.

We use the implicit stiff solver `ode15s` in Matlab in all of the examples shown above. Unfortunately, even that is not enough. The extremely high stiffness possible in these problems can cause difficulties with rounding (computer arithmetic) errors in the linear algebra used at each time step of the implicit solver, and even in the evaluation of the right hand side of the ODEs (1.5) themselves. These typically involve summing two groups of positive terms and subtracting the results, which introduces relatively large rounding errors when the two numbers are almost equal. The rounding errors can be large compared to the local error estimates used for efficient time step control, making it unreliable and erratic, forcing the algorithm to take far more steps (and computer time) than it needs to. When applying the ODE solver directly to the original ODE system (1.5), this problem is severe in the Example 1 tests above, while the Example 2 tests are reasonably well-behaved.

Fortunately the centre manifold analysis in Section 3 and earlier work [5] for the Becker-Döring coagulation-fragmentation ODE system, suggests a way to reduce rounding error issues. Instead of solving (1.5) directly we use the equivalent centre manifold system (3.8). Results are obtained far more efficiently in the Example 1 tests with little impact on the Example 2 tests. This is partly because the important first equation of (3.8) has no cancellation of terms to worry about, since it is a sum of same-sign quantities as seen in (3.9). One can either apply the solver directly to the ODE system (3.8) and solve for (x, c_2, \dots, c_n) , or follow [5] more

closely and apply it to the equivalent differential algebraic system

$$\sum_{j=1}^n jc'_j = f\left(\sum_{j=1}^n jc_j, y\right), \quad y' = By + g\left(\sum_{j=1}^n jc_j, y\right),$$

and solve for (c_1, c_2, \dots, c_n) . Both variants are equally efficient in tests.

5 Conclusions

The truncated system (1.5) appears to approximate the behaviour of the full infinite system well. The centre manifold asymptotic behaviour given in Theorem 3.1 appears clearly in the numerical experiments of the previous section. For mass conserving problems the approximate centre manifold quantities and (4.2) provide a good estimate of how long the truncated system conserves mass for, which is a measure of its range of validity as an approximation of the original infinite system. For problems with gelation like Example 2, plots like those in Figure 4 to Figure 7 with information from Theorem 3.1 reveal how the truncated system will behave for different choices of initial mass and system size.

For the infinite system a number of intriguing questions remain about the long-term behaviour in the presence of gelation, such as in Example 2 with $\alpha > 1$. In infinite systems without gelation, but with a maximum possible equilibrium density, solutions generally converge weakly to the maximum density equilibrium. When gelation is also present, does the solution converge to 0 or to some other equilibrium?

Acknowledgement: Sadly, Jack Carr died in 2016 after a short illness, during which he continued to work so that this article could be finished. His enthusiasm, wide knowledge and deep insights into the mathematics of these problems made it both a pleasure and a privilege to work with him.

References

- [1] J.P. Bourgade and F. Filbet, *Convergence of a finite volume scheme for coagulation-fragmentation equations*, Mathematics of Computation, **77**, number 262, pages 851-882, 2008.
- [2] J.M. Ball and J. Carr, *The discrete coagulation-fragmentation equations: existence, uniqueness, and density conservation*, J. Statist. Phys., **61**, pages 203-234, 1990.
- [3] J. Carr, *Asymptotic behaviour of solutions to the coagulation-fragmentation equations. I. The strong fragmentation case*, Proc. Roy. Soc. Edinburgh Sect. A, **121**, number 3-4, pages 231-244, 1992.
- [4] J. Carr, Applications of Centre Manifold Theory, Springer-Verlag, 1981.
- [5] J. Carr, D.B. Duncan and C.H. Walshaw, *Numerical approximation of a metastable system*, IMA Journal of Numerical Analysis, **15**, pages 505-521, 1995.

- [6] F.P. da Costa, *Existence and uniqueness of density conserving solutions to the coagulation-fragmentation equations with strong fragmentation*, Journal of Mathematical Analysis and Applications, **192**, pages 892–914, 1995.
- [7] F.P. da Costa, *A finite-dimensional dynamical model for gelation in coagulation processes*, J. Nonlinear Sci. **8**, number 6, pages 619–653, 1998.
- [8] F.P. da Costa, H.J. van Roessel and J.A.D. Wattis, *Long-time behaviour and self-similarity in a coagulation equation with input of monomers*, Markov Processes Relat. Fields **12**, pages 367–398, 2006.
- [9] M. Escobedo, S. Mischler and B. Perthame, *Gelation in coagulation and fragmentation models*, Comm. Math. Phys., **231**, number 1, pages 157–188, 2002.
- [10] M. Escobedo, Ph. Laurenot, S. Mischler and B. Perthame, *Gelation and mass conservation in coagulation-fragmentation models*, Journal of Differential Equations, **195**, pages 143–174, 2003.
- [11] P. Glendinning, *Stability, Instability and Chaos: An Introduction to the Theory of Non-linear Differential Equations*, Cambridge University Press, 1994.
- [12] R. Kollar, K. Bodova, J. Nosek and L. Tomaska, *Mathematical model of alternative mechanism of telomere length maintenance*, Physical Review E, **89**, 032701, 2014.
- [13] F. Leyvraz and H.R. Tschudi, *Singularities in the kinetics of coagulation processes*, Journal of Physics. A., **12**, number 12, pages 3389–3405, 1981.
- [14] J.B. McLeod, *On an infinite set of non-linear differential equations*, Quart. J. Math. Oxford Ser. (2), **13**, pages 119–128, 1962.